Meson production in air showers and the search for light exotic particles

M. Kachelrieß and J. Tjemsland

Institutt for fysikk, NTNU, Trondheim, Norway

Abstract

Decays of mesons produced in cosmic ray induced air showers in Earth's atmosphere can lead to a flux of light exotic particles which can be detected in underground experiments. We evaluate the energy spectra of the light neutral mesons π^0, η, ρ^0, ω, ϕ and J/ψ produced in interactions of cosmic ray protons and helium nuclei with air using QCD inspired event generators. Summing up the mesons produced in the individual hadronic interactions of air showers, we obtain the resulting fluxes of undecayed mesons. As an application, we re-consider the case of millicharged particles created in the electromagnetic decay channels of neutral mesons.

1. Introduction

While overwhelming evidence has been accumulated for the existence of dark matter (DM) from astrophysical and cosmological observations, the experimental searches for such particles in direct detection experiments have not been successful yet. Combined with the null results in searches for new physics at the LHC, this indicates that new particles with masses below the TeV scale are only weakly coupled to the standard model. The prime candidate for such a DM particle, a thermal relic with mass around the weak scale, has been constrained severely and is on the eve of being excluded: For instance, the upper limit on the annihilation cross section obtained by the Fermi-LAT collaboration using dwarf galaxies excludes thermal relics with masses below $\sim 100\,\mathrm{GeV}$ [1], while model dependent limits from antiproton data are typically even more stringent [2, 3]. Therefore, both model building and experimental searches have expanded their phenomenological scope considerably the last decade, investigating e.g. light DM particles with masses in the sub-GeV range.

Traditionally, this mass range has been considered to be inaccessible to direct detection experiments, since the recoil energy of a DM particle with typical Galactic velocities, $v \sim 10^{-3}c$, is below the threshold energy of such experiments. However, Refs. [4, 5] recently pointed out that cosmic rays (CRs) colliding with DM can up-scatter them, leading to a significantly increased DM flux above the threshold energy of direct detection experiments. Another generic source of light DM particles are CR interactions in the atmosphere of the Earth [6–11]. If mesons produced in these interactions decay partially into DM, an energetic DM flux that can be detected in underground experiments results. While the up-scattering

mechanism relies on a sufficiently large abundance of the DM particle considered, CR interactions in the atmosphere depend only on the well-known flux of incident cosmic rays. This mechanism can moreover produce other long-lived exotic particles, thereby extending the reach of searches for new physics.

In this work, we re-evaluate the atmospheric fluxes of undecayed π^0, η, ρ, ω, ϕ and J/ψ mesons, which we denote collectively by m. In a previous study by Plestid *et al.* [12], these fluxes were computed using parametrisations for the relevant production cross sections in pp collisions. Here, we improve upon this in several aspects: First, we use QCD inspired event generators to model the particle production in single hadronic interactions. This allows us to account for the contribution of helium in the CR primary flux as well as for the effect of air as target nuclei. Comparing the results of different event generators we obtain an estimate for the uncertainties of their predictions. Moreover, we model the complete hadronic air shower by considering interactions of secondaries such as $\pi^{\pm}p \to mX$ and $K^{\pm}p \to mX$. Our main result is thus an improved description of the atmospheric flux of undecayed mesons produced in air showers. Our tabulated results can be used to evaluate the flux of exotic particles produced by atmospheric meson decays within generic extensions of the standard model[1]. Possible applications include, for instance, the decay of π^0 and η mesons into a pair of DM particles through a bosonic mediator [11], and the case of millicharged DM that couples to the Standard Model (SM) via a photon [13]. As an illustration for the application of our atmospheric flux of undecayed mesons, we consider the production of a generic millicharged particle (mCP) and compare our results with those of Ref. [12]. Such particles arise naturally through, e.g., the kinetic mixing between the SM photon and a dark photon [14–18]. The possible mass-to-charge ratio $m/\varepsilon e$ of models in which the DM is charged are already strongly constrained by astrophysical processes as well as ground based experiments, see e.g. Refs. [19–21]. However, these limits can be avoided, if the charged component is unstable on cosmological time scales or constitutes only a small part of the total DM abundance. Therefore, DM theories with a sub-dominant charged component in a hidden sector have attracted attention, for recent reviews see Refs. [22, 23]. An additional motivation for such models is the EDGES anomaly which can be explained in a small window in parameter space close to the limits from direct detection experiments [24, 25].

This paper is structured as follows. In section 2, we first compare the meson production cross sections calculated using various QCD inspired event generators to experimental data, and compute next the atmospheric flux of undecayed neutral mesons. As an example for the applicability of the tabulated fluxes, we re-evaluate the flux of mCPs from atmospheric meson decays in section 3. Finally, a summary is given in section 4.

2. Meson production in air showers

High energy cosmic rays entering the atmosphere interact with air nuclei. The produced long-lived hadrons will in turn interact with other air nuclei, thus creating a so-called hadronic air shower. The short-lived particles, on the other hand, may decay. About 1/3

[1]Tables for the integrated meson fluxes are attached to the arxiv submission.

of the energy is transferred in each generation of the air shower into the electromagnetic component, mainly via the decay of short-lived mesons. Thus, the decay of mesons in a hadronic air shower may be a promising detection channel for exotic particles that interact with the SM via a photon, such as mCPs. To describe the hadronic interactions, we utilize the QCD inspired event generators DMPJET III 19.1 [26–28], Pythia 8.303 [29], QGSJET II-04 [30, 31], Sibyll 2.3d [32], and UrQMD 3.4 [33]. The focus will be on DPMJET and Sibyll which are event generators widely used in the field of CR physics. An exception is the production of J/ψ mesons, where we rely on the event generator Pythia which is focused on accelerator physics.

2.1. Production cross sections

Parametrisations of hadronic interactions relying on empirical scaling laws are often used as an efficient tool to reproduce inclusive quantities like total cross sections. The use of such parametrisations becomes, however, dangerous when they are extrapolated outside the kinematical range of the data they are based on. Moreover, such parametrisations are generally not available for the cases where nuclei are employed as CR primaries or targets. In this work, we use therefore Monte Carlo event generators in the description of hadronic interactions to compute the atmospheric meson fluxes. While this approach avoids the disadvantages of parametrisations, it has also its own drawbacks: In particular, QCD inspired event generators cannot be used below a minimal energy, which is typically in the range of 5–10 GeV/n of the projectile in the lab frame. While this implies that most of the CR interactions in the atmosphere cannot be simulated using these event generators, we will see that the bulk of the produced mesons is still well described due to the strong suppression of particle production near threshold.

To test the event generators, we compare in Fig. 1 the production cross sections of η, ρ, ω and ϕ mesons computed using DPMJET, Sibyll and UrQMD to the experimental data on the inclusive meson production cross section $\sigma_{pp\to mX}$ in pp collisions from Refs. [34–36]. Additionally, we show the parametrisations used in Ref. [12]. There is overall a good agreement between the experimental data and the predictions of the event generators. We do, however, note a few deficiencies: First, we see that UrQMD overproduces ϕ mesons by an energy-dependent factor. Next, we note that DPMJET overproduces ρ and ω mesons. In this case, we obtain a good description of the data by rescaling[2] the production cross sections of ρ and ω mesons by a factor 0.5. Finally, we comment on the case of J/ψ mesons: DPMJET predicts a J/ψ production cross section that is 3–4 orders of magnitude below those of Sibyll and Pythia, indicating that the most important production channels of this meson are not included in this event generator. We have therefore decided to focus in the following mainly on DPMJET and Sibyll computing the production of η, ρ, ω and ϕ mesons, as they describe well the experimental data (after the rescaling) and are reasonably fast. The other aforementioned event generators will be used as basis for comparison. In addition, Pythia will be used to describe the production of J/ψ mesons.

[2] A proper solution which would require to increase appropriately the production cross sections of other particles as, e.g., a_0 and f_0 mesons is planned for a future version of DPMJET [37].

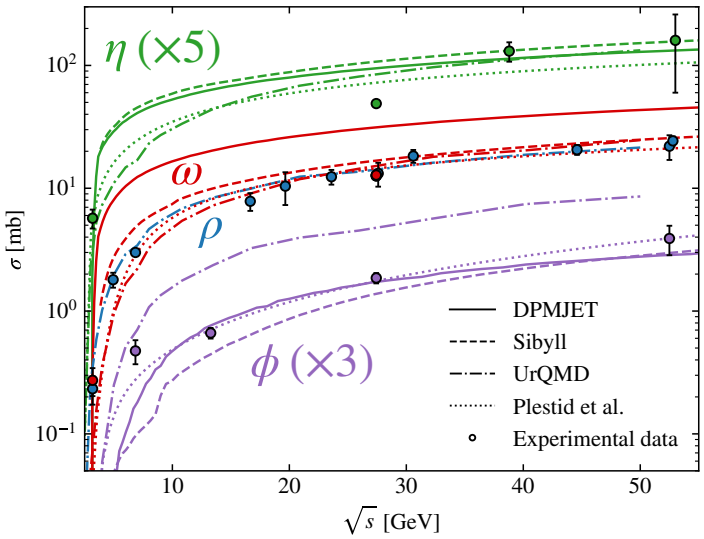

Figure 1: The total production cross section of η (green), ρ (blue), ω (red) and ϕ (purple) mesons computed using DPMJET (solid), Sibyll (dashed) and UrQMD (dashed dotted) is compared to experimental data on the total inclusive cross sections from Refs. [34–36]. The parametrisations used in Ref. [12] are shown for comparison (dotted). The η and ϕ cross sections are multiplied by a constant factor to make the figure clearer. In the case of Sibyll and DPMJET, the ρ and ω fluxes are close to overlapping, thus only the ω flux is shown.

2.2. Flux of undecayed mesons

Next we compute the flux of undecayed mesons of the types π^0, η, ρ^0, ω, ϕ and J/ψ in hadronic air showers induced by cosmic ray proton and helium nuclei using a self-written Monte Carlo code in which the interactions of hadrons are handled using QCD inspired event generators. We consider He, p, $\pi^\pm$ and $K^\pm$ as stable[3] projectiles and nitrogen as target[4]. All short-lived particles that are not treated as a projectile are set to decay using the decay subroutines in Pythia. Since we are mainly interested in the integrated meson fluxes as a function of energy, we neglect the direction of the produced particles, keeping all down-going particles. Moreover, practically all primaries above the production threshold will interact, and we can therefore ignore the finite extension of the atmosphere. Finally, we can neglect the tertiary contribution to meson production due to the electromagnetic shower component, because the average energy per produced secondary is for photons/electrons smaller than for mesons and the cross sections for, e.g., photo-pion production are suppressed relative

[3]At low energies, charged mesons will decay, implying that this treatment will lead to an overestimation of the meson yields. Considering for concreteness $E_c = 30$ GeV [38] as a hard cut-off and $\pi^\pm$ as primaries, we can estimate that there will only be an effect at meson energies $E < (m_N^2 + m_{\pi^\pm}^2 + 2m_N E_c)^{1/2} - m_N - m_{\pi^\pm} \simeq 6.5\,\text{GeV}$. The effect will be small as there will be a large contribution from charged pions at higher energies. In particular, the effect on interesting observables in the production of exotic particles above detector thresholds will be negligible.

[4]With Pythia, we consider only pp interactions and take into account the helium flux by rescaling the proton flux appropriately.

to electromagnetic ones. For the primary CR fluxes, we use the parametrisations fitted to proton and helium data from AMS-02, DAMPE and CREAM given in Ref. [3].

Before proceeding, the chosen energy cutoffs should be discussed. We use 2 GeV/n as a low-energy threshold for DPMJET, QGSJET and UrQMD, while we set 8 GeV/n and 60 GeV/n for Sibyll[5] and Pythia, respectively. These energy cutoffs should be compared to the threshold energy in the interaction $pp \to pp\pi$ which are 1.2, 2.2, 2.8, 3.5 and 12 GeV for π^0, η, ρ^0, ω, ϕ and J/ψ mesons, respectively. Thus the chosen cut-off in DPMJET, QGSJET and UrQMD is sufficiently small for all considered mesons except for the π^0; the results for this meson must therefore be considered with care[6]. Even more, the threshold suppression in the production cross section will at some point be stronger than the power law increase in the primary CR flux. This means that even if Sibyll cannot describe most particle interactions, it will still describe the bulk of produced mesons more massive than π^0. Likewise, Pythia will describe well the atmospheric J/ψ flux, as is readily seen by Fig. 2 in Ref. [12].

The main contribution to the meson production comes from the first interaction at the top of the atmosphere, because the cosmic ray flux is a steeply falling function of energy, $\Phi^{\rm CR}(E) \propto E^{-2.7}$. Moreover, the cosmic ray flux is at low energies dominated by protons. Therefore, we start by plotting in Fig. 2 the integrated meson fluxes from pp interactions weighted by the cosmic ray flux $\Phi^{\rm CR}(E) \simeq \Phi_p(E) + 4\Phi_{\rm He}(E/4)$ as a simple benchmark case. Note that the production yields of ρ and ω mesons are divided by a factor 2 in the case of DPMJET, as described in the previous subsection. As a basis for comparison, we plot also the result obtained using QGSJET (only for π^0), Pythia (only ϕ and J/ψ) and UrQMD (only π^0, η, ρ and ω). The effect of the chosen cutoffs are clearly visible: Lowering the energy threshold extends the power law to lower energies and increases the flux of produced mesons at low energies. For instance, the maximum of the π^0 flux computed with Sibyll is suppressed by a factor $\simeq 10$ compared to DPMJET. This effect is smaller for heavier mesons, because of their increased production threshold. The remaining overall differences for heavier mesons can be explained by the differences in the computed production cross sections (see section 2.1). The differences between DPMJET and Sibyll (for mesons heavier than π^0) capture well the uncertainties in the different event generators, which are below a factor 2–3.

In Fig. 3, the computed undecayed meson fluxes from hadronic air showers are shown. The effect of including the cascade leads to a noticeable increase in the flux at low meson energies, and shifts its maximum slightly to smaller energies. However, the difference in the fluxes for Sibyll and DPMJET are larger than the gain in including the complete cascade, even at low energies. These effects are more visible in Fig. 4. Here, the ratios of the meson fluxes of π^0, η, ρ and ω from pN initiated air showers, $\Phi_{pN}^{\rm cascade}$, and from a single pp interaction

[5]The chosen threshold for Sibyll is lower that the intended validity range, but as seen in subsection 2.1 Sibyll describes well the production cross sections down to $E_{\rm lab} \simeq 6.4$ GeV.

[6]Note that we consider π^0 mesons only for completeness. As we will see in the next section, exotic particle production from π^0 decays is already strongly constrained by collider experiments. It is therefore doubtful that the decay of π^0 in atmospheric cascade can give leading constraints.

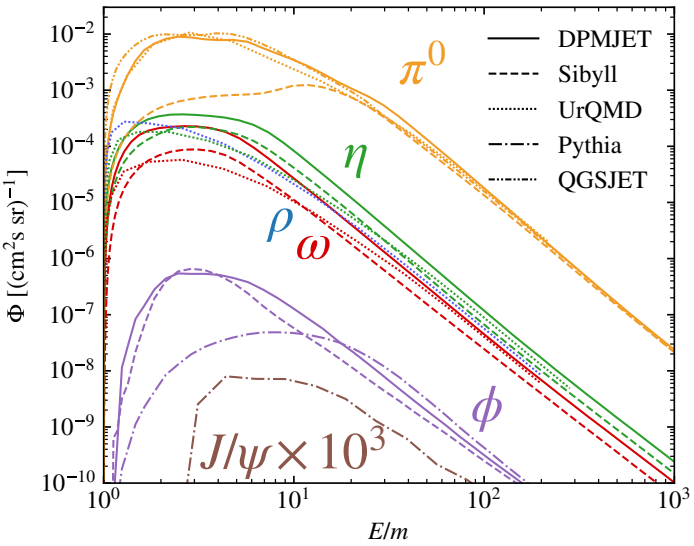

Figure 2: The flux of produced π^0 (orange), η (green), ρ (blue), ω (red), ϕ (purple) and J/ψ (brown) mesons in pp and Hep collisions at the top of the atmosphere are computed using DPMJET (solid lines), Sibyll (dashed), QGSJET (dashed-dotted-dotted), Pythia (dashed-dotted) and UrQMD (dotted). Only a selection of meson species are shown for different event generators to make the figure clearer. In the case of Sibyll and DPMJET, the ρ and ω fluxes are close to overlapping, thus only the ω flux is shown.

at the top of the atmosphere, Φ_{pp}, are shown. For comparison, the ratio $\Phi_{pp}^{\text{cascade}}/\Phi_{pp}$ of the fluxes from a pp air shower and a single pp interaction is shown for Pythia. Interestingly, the effect of including target nuclei lowers the flux at large energies, because the kinetic energy in the center of mass frame of the interaction is effectively reduced. This effect is larger for DPMJET than for Sibyll.

The meson fluxes in Fig. 3 differ significantly[7] from those computed in Ref. [12]: For small meson energies, our fluxes are suppressed more strongly, leading to a difference of about one order of magnitude around the maximum. Meanwhile, for large meson energies the differences are small and consistent with the differences in the production cross sections discusses in subsection 2.1.

3. Application: Atmospheric production of millicharged particles

In this section we analyze the production of mCP from the intermediate meson decays in the atmosphere. This serves as a (conservative) benchmark model for mCP, with the advantage of having only two free parameters: its mass m and charge $e\varepsilon$. We take into account the decays $\pi^0 \to \{\bar{\chi}\chi, \bar{\chi}\chi\gamma\}$, $\eta \to \{\bar{\chi}\chi, \bar{\chi}\chi\gamma\}$, $\rho \to \bar{\chi}\chi$, $\omega \to \{\bar{\chi}\chi, \bar{\chi}\chi\pi^0\}$, $\phi \to \bar{\chi}\chi$

[7] One should note that the meson fluxes found in Ref. [12] were considered as *a useful byproduct*, while their main result—the integrated flux of mCPs above detector thresholds—are mostly sensitive to the total production cross sections.

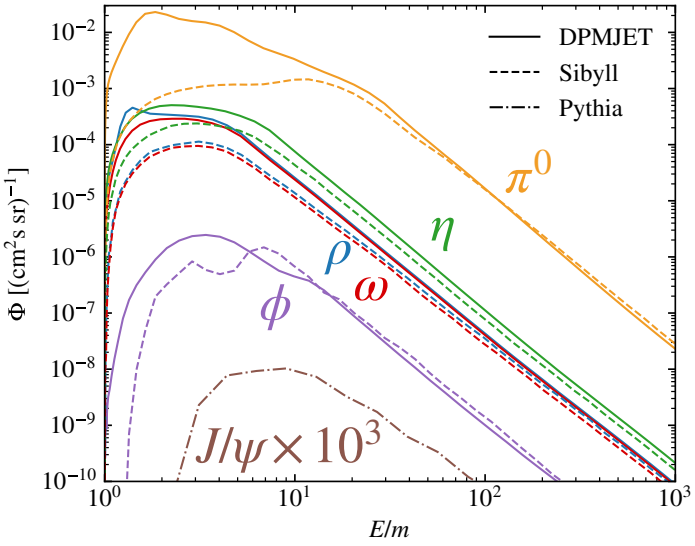

Figure 3: Meson flux produced in air showers using DPMJET, Sibyll and Pythia (only J/ψ). The line-styles are the same as in Fig. 2.

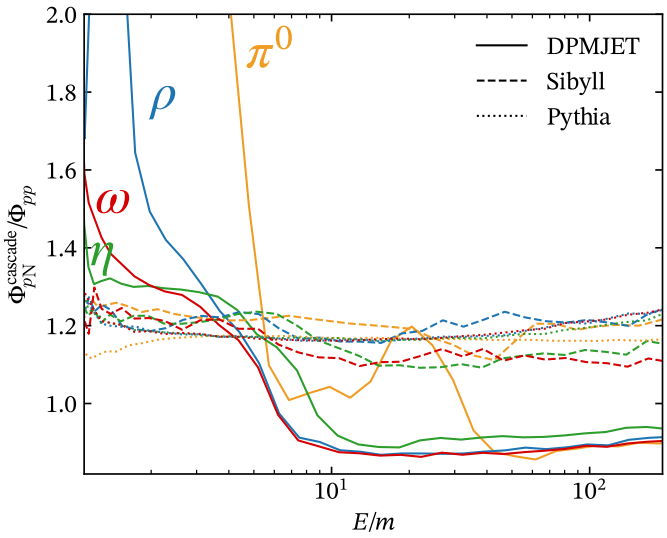

Figure 4: Ratio $\Phi_{pN}^{\rm cascade}/\Phi_{pp}$ of the meson fluxes in pN air showers and a single pp collision computed using DPMJET (solid lines) and Sibyll (dashed lines). For comparison, $\Phi_{pp}^{\rm cascade}/\Phi_{pp}$ of the fluxes from a pp air shower and a single pp interaction is shown in the case of Pythia. The color-scheme indicating the various mesons are the same as in the previous figures.

and $J/\psi \to \bar{\chi}\chi$. The corresponding branching ratios are estimated by rescaling the dilepton and diphoton branching ratios, as explained in Appendix A. We handle the $1 \to 3$ decays using the decay subroutines in Pythia 8, whereas the momentum distribution in the $1 \to 2$ decays is taken to be monoenergetic and isotropic in the rest frame of the mother particle.

The integrated mCP fluxes computed using DPMJET and Sibyll are shown in Fig. 5 as a function of the mCP mass. The result obtained for J/ψ using Pythia is also shown. The step-like behaviour arises from the various thresholds at $m_m/2$, as indicated in the figure. In addition, we show the integrated mCP flux with a cutoff at the Lorentz factor $\gamma_{\rm mCP} = E/m_{\rm mCP} = 6$, which corresponds approximately to the cut-off of the Super-Kamiokande experiment used in their search for relic supernova neutrinos [39] (see Appendix B): The upper line of the shaded gray region corresponds to the mCP flux for $\gamma_{\rm mCP} > 6$ calculated with DPMJET, while the lower line uses Sibyll.

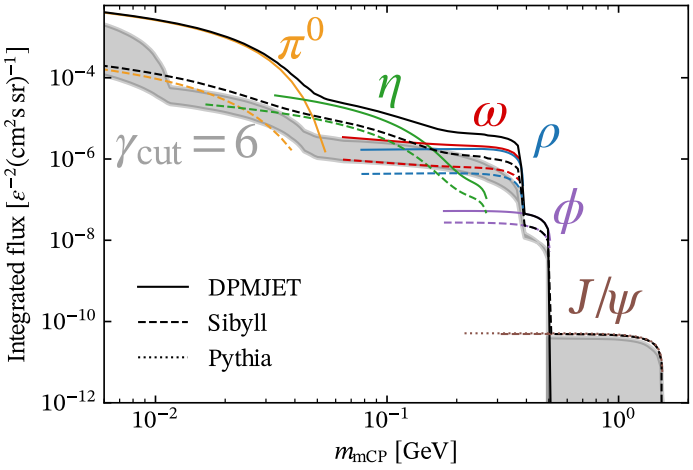

Figure 5: The integrated flux of mCPs from meson decays in the atmosphere for varying mCP mass using DPMJET (solid), Sibyll (dashed) and Pythia (dotted; only J/ψ) are shown in black. The contributions from the different meson species are indicated using the same colors as in Fig. 2. The shaded gray region indicates the integrated flux above $\gamma_{\rm cut} = 6$.

For completeness, we also show an exclusion plot using data from Super-Kamiokande [39] employing the procedure introduced in Ref. [12]. A brief description of the procedure is given in Appendix B. The result is shown in Fig. 6 where it is compared to a minor subset of existing limits (see e.g. Ref. [40] for additional bounds). Intriguingly, the limit set by atmospheric mesons is comparable to the existing strong limit set by the ArgoNeuT experiment [41]. Note also that neutrino detectors may have a significantly lower threshold energy than used here for Super-Kamiokande. For example, the Borexino detector has in principle a threshold of $\sim$ 200 keV only limited by the natural presence of ^{14}C [42]. Thus, the limit set by atmospheric mesons could in principle be significantly improved. This strengthens the importance of an accurate description of atmospheric mesons, and motivates future work on using neutrino detectors to search for exotic physics as introduced

in Ref. [12].

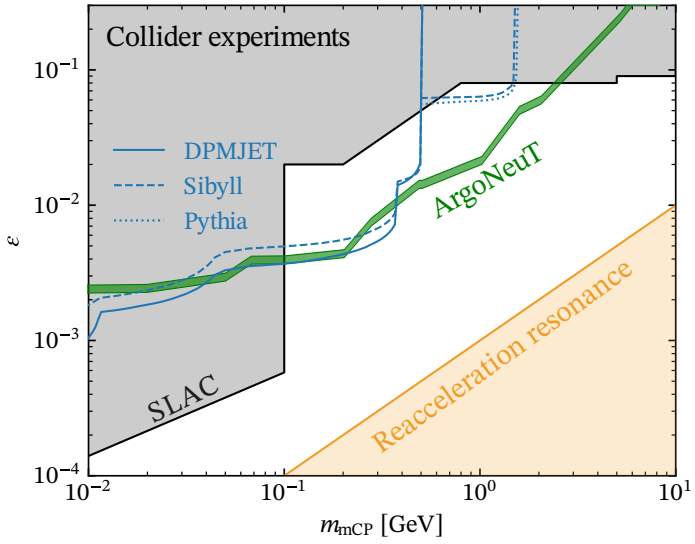

Figure 6: The upper limit in (m, q)-parameter space of mCPs set by the non-detection supernova neutrino events in Super-Kamiokande [39]. The result is similar to that of Ref. [12]. To put it in perspective, the upper limit set by various collider experiments [43–47] and the ArgoNeuT experiment [41] are shown. The strong limit below the π^0 threshold comes from the search for millicharged particles at SLAC [43]. The lower limit set by the reacceleration condition [21] is only valid if the mCPs make up more that $\sim 10^{-6}$ of the relic abundance.

4. Summary

In this work we have computed the flux of atmospheric mesons by simulating hadronic air showers using the event generators DPMJET III 19.1, Pythia 8.303, QGSJET II-04, Sibyll 2.3d and UrQMD 3.4. The emphasis was put on Sibyll and DPMJET, as they describe well the total production cross sections and are fast. Moreover, the difference between these two event generators may serve as an estimate for the theoretical uncertainties of our flux predictions. We have focused on the production of mesons with large electromagnetic decay channels, π^0, η, ρ, ω, ϕ and J/ψ.

This work was motivated by Ref. [12], where the meson fluxes produced in pp collisions at the top of the atmosphere were computed by fitting various parametrisations to measurements of meson production cross sections. The obtained fluxes were in turn used to set constraints on generic BSM models with a (meta-)stable millicharged component. Our results are in good agreement with those of Ref. [12]. The largest differences (up to orders of magnitude at low meson energies) arise due to the different treatment of the cross sections. The Monte Carlo approach has several advantages compared to using parametrisations: secondary interactions as well as the effect of interacting nuclei can be taken into account. Moreover, no assumption has to be made on the momentum dependence of the differential

cross section. By comparing the results obtained using DPMJET and Sibyll for mesons more massive than π^0 we found an estimated uncertainty of the theoretical predictions of a factor 2–3. This uncertainty is larger than the changes resulting from adding secondary interactions and simulating helium as projectile and nitrogen as target. The effect of the larger interaction threshold in Sibyll compared to DPMJET is small for all considered mesons, except for π^0 at low meson energies.

Our tabulated results can be used to evaluate the flux of exotic particles produced by atmospheric meson decays within generic extensions of the standard model. As an example, we re-considered the production of millicharged particles, and found that their production in atmospheric meson decays can set leading constraints in the possible charge-to-mass ratio. The in principle lower thresholds for neutrino experiments is a strong motivation for continuing the study of exotic particles produced in meson decay in the atmosphere.

Acknowledgments

We would like to thank Anatoli Fedynitch for helpful comments on DPMJET III.

Appendix A. Meson branching ratios into millicharged particles

The branching ratios of mesons m into mCPs χ can be found by rescaling the branching ratios of their electromagnetic decay channels into charged leptons $l^{\pm}$. The direct decay of mesons into mCPs, $m \to \bar{\chi}\chi$, the Dalitz decays of pseudoscalar mesons, $P \to \bar{\chi}\chi\gamma$, and the three-particle decay of vector mesons, $V \to \bar{\chi}\chi P$ will give the dominant contributions to the mCP production in hadronic interactions. We use for evaluation[8] of the relevant branching ratios the experimental values given by the particle data group [48].

The branching ratio of a direct meson decay into two mCPs, $m \to \bar{\chi}\chi$, can be found by rescaling the dilepton branching ratio [49] as

$$\frac{\mathrm{BR}\,(m \to \bar{\chi}\chi)}{\mathrm{BR}\,(m \to l^+l^-)} = \varepsilon^2 \sqrt{\frac{1-4m_\chi^2/m_m^2}{1-4m_l^2/m_m^2}} \frac{1+2m_\chi^2/m_m^2}{1+2m_l^2/m_m^2}. \tag{A.1}$$

In this work, we consider the direct decays of π^0, η, ρ, ω, ϕ and J/ψ.

The branching ratio of a pseudoscalar mesons into a photon and a mCP pair, $P \to \gamma\bar{\chi}\chi$, can be computed by rescaling the diphoton branching ratio [49] as

$$\frac{\mathrm{BR}\,(P \to \gamma\bar{\chi}\chi)}{\mathrm{BR}\,(m \to \gamma\gamma)} = \frac{2\alpha\varepsilon^2}{3\pi} \int_{4m_\chi^2}^{m_m^2} \mathrm{d}q^2 \sqrt{1-\frac{4m_\chi^2}{q^2}} \left(1+2\frac{m_\chi^2}{q^2}\right) \frac{1}{q^2} \left(1-\frac{q^2}{m_m^2}\right)^3 |F_m(q^2)|^2, \tag{A.2}$$

with $F_m(q^2)$ being the meson form factor and q^2 the invariant mass of the virtual photon. Likewise, the branching ratio for a vector (pseudoscalar) meson into two mCPs and a

[8] We use, except for π^0 decays, muons for comparisons, $l^{\pm} = \mu^{\pm}$.

pseudoscalar (vector) meson is given by

$$\frac{\mathrm{BR}\,(m \to A\bar{\chi}\chi)}{\mathrm{BR}\,(m \to \gamma\gamma)} = \frac{\alpha\varepsilon^2}{3\pi} \int_{4m_\chi^2}^{(m_m - m_\chi)^2} \mathrm{d}q^2 \sqrt{1 - \frac{4m_\chi^2}{q^2}} \left(1 + 2\frac{m_\chi^2}{q^2}\right) \frac{1}{q^2} \times \left[\left(1 + \frac{q^2}{m_m^2 - m_A^2}\right)^2 - \frac{4m_m^2 q^2}{(m_m^2 - m_A^2)^2}\right]^{3/2} |F_m(q^2)|^2. \tag{A.3}$$

In this work, we consider the three-body decays $\pi^0 \to \gamma\bar{\chi}\chi$, $\eta \to \gamma\bar{\chi}\chi$ and $\omega \to \pi^0\bar{\chi}\chi$. We take into account the meson form factors using the parametrisations from Refs. [48, 49]:

$$F_{\pi^0}(q^2) \approx 1 + q^2 b_{\pi^0}, \quad b_{\pi^0} = (5.5 \pm 1.6)\ \mathrm{GeV}^{-2}, \tag{A.4}$$

and

$$F_i(q^2) = \left(1 - \frac{q^2}{\Lambda_i^2}\right)^{-1}, \quad \begin{aligned} \Lambda_\eta &= (0.716 \pm 0.011)\ \mathrm{GeV}, \\ \Lambda_\omega &= 0.65\ \mathrm{GeV}. \end{aligned} \tag{A.5}$$

Appendix B. Upper limit from neutrino experiments

Water Cherenkov detectors like Super-Kamiokande [39] search for the light signal emitted by the relativistic charged particles. Therefore the light signal emitted by the scattered electrons in the elastic interactions $\chi e^- \to \chi e^-$ can be used to constrain the flux of mCP with scatterings within a kinetic energy range $T_{\mathrm{min}} < T < T_{\mathrm{max}}$. This leads to a "windowed cross section" for mCP-electron interactions that can approximated as

$$\tilde{\sigma}_{e\chi}(\gamma_\chi) = \int_{q^2_{\mathrm{min}}}^{q^2_{\mathrm{max}}} \frac{\mathrm{d}\sigma_{e\chi}}{\mathrm{d}q^2}\,\mathrm{d}q^2 \approx \frac{2\pi\alpha^2\varepsilon^2}{2T_{\mathrm{min}}m_e}\left(1 - \frac{T_{\mathrm{min}}}{T_{\mathrm{max}}}\right)\Theta(\gamma_\chi - \gamma_{\mathrm{cut}}) \tag{B.1}$$

with $\gamma_{\mathrm{cut}} \approx 0.6\sqrt{2T_{\mathrm{min}}/m_e} + 0.4\sqrt{2T_{\mathrm{max}}/m_e}$ [12]. The expected number of events is then

$$N_{e\chi} \approx N_e t \int_{\gamma_{\mathrm{cut}}}^{\infty} \tilde{\sigma}_{e\chi}(\gamma_\chi)\frac{\mathrm{d}\Phi_\chi}{\mathrm{d}\gamma_\chi}\,\mathrm{d}\gamma_\chi \tag{B.2}$$

with N_e as the number of electrons in the detector and t as the sampling period. For Super-Kamiokande, $T_{\mathrm{min}} = 16$ MeV and $T_{\mathrm{max}} = 88$ MeV [39], corresponding to $\gamma_{\mathrm{cut}} \approx 6$ [12]. Since the event shape of mCPs is similar to that of the supernova background (see Fig. 10 in Ref. [12]), one can make use of the analysis performed in Ref. [39] for Super-Kamiokande, which essentially leads to an exclusion of ~ 4 events are excluded with 90 % CL.

References

[1] M. Ackermann, et al., Searching for Dark Matter Annihilation from Milky Way Dwarf Spheroidal Galaxies with Six Years of Fermi Large Area Telescope Data, Phys. Rev. Lett. 115 (23) (2015) 231301. arXiv:1503.02641, doi:10.1103/PhysRevLett.115.231301.

[2] N. Fornengo, L. Maccione, A. Vittino, Dark matter searches with cosmic antideuterons: status and perspectives, JCAP 1309 (2013) 031. arXiv:1306.4171, doi:10.1088/1475-7516/2013/09/031.
[3] M. Kachelrieß, S. Ostapchenko, J. Tjemsland, Revisiting cosmic ray antinuclei fluxes with a new coalescence model, JCAP 08 (2020) 048. arXiv:2002.10481, doi:10.1088/1475-7516/2020/08/048.
[4] T. Bringmann, M. Pospelov, Novel direct detection constraints on light dark matter, Phys. Rev. Lett. 122 (17) (2019) 171801. arXiv:1810.10543, doi:10.1103/PhysRevLett.122.171801.
[5] Y. Ema, F. Sala, R. Sato, Light Dark Matter at Neutrino Experiments, Phys. Rev. Lett. 122 (18) (2019) 181802. arXiv:1811.00520, doi:10.1103/PhysRevLett.122.181802.
[6] A. Kusenko, S. Pascoli, D. Semikoz, New bounds on MeV sterile neutrinos based on the accelerator and Super-Kamiokande results, JHEP 11 (2005) 028. arXiv:hep-ph/0405198, doi:10.1088/1126-6708/2005/11/028.
[7] P.-f. Yin, S.-h. Zhu, Detecting light long-lived particle produced by cosmic ray, Phys. Lett. B 685 (2010) 128–133. arXiv:0911.3338, doi:10.1016/j.physletb.2010.01.067.
[8] P.-K. Hu, A. Kusenko, V. Takhistov, Dark Cosmic Rays, Phys. Lett. B768 (2017) 18–22. arXiv:1611.04599, doi:10.1016/j.physletb.2017.02.035.
[9] C. Argüelles, P. Coloma, P. Hernández, V. Muñoz, Searches for Atmospheric Long-Lived Particles (2019). arXiv:1910.12839.
[10] P. Coloma, P. Herández, V. Muñoz, I. M. Shoemaker, New constraints on Heavy Neutral Leptons from Super-Kamiokande data (2019). arXiv:1911.09129.
[11] J. Alvey, M. Campos, M. Fairbairn, T. You, Light Dark Matter from Inelastic Cosmic Ray Collisions, Phys. Rev. Lett. 123 (26) (2020) 261802, [Phys. Rev. Lett.123,261802(2019)]. arXiv:1905.05776, doi:10.1103/PhysRevLett.123.261802.
[12] R. Plestid, V. Takhistov, Y.-D. Tsai, T. Bringmann, A. Kusenko, M. Pospelov, New Constraints on Millicharged Particles from Cosmic-ray Production (2 2020). arXiv:2002.11732.
[13] A. Y. Ignatiev, V. A. Kuzmin, M. E. Shaposhnikov, Is the Electric Charge Conserved?, Phys. Lett. B 84 (1979) 315–318. doi:10.1016/0370-2693(79)90048-0.
[14] L. B. Okun, M. B. Voloshin, V. I. Zakharov, Electrical neutrality of atoms and Grand Unification models, Phys. Lett. 138B (1984) 115–120. doi:10.1016/0370-2693(84)91884-7.
[15] H. Georgi, P. H. Ginsparg, S. Glashow, Photon Oscillations and the Cosmic Background Radiation, Nature 306 (1983) 765–766. doi:10.1038/306765a0.
[16] B. Holdom, Two U(1)'s and Epsilon Charge Shifts, Phys. Lett. 166B (1986) 196–198. doi:10.1016/0370-2693(86)91377-8.
[17] M. I. Dobroliubov, A. Yu. Ignatiev, Millicharged particles, Phys. Rev. Lett. 65 (1990) 679–682. doi:10.1103/PhysRevLett.65.679.
[18] P. Fayet, Extra U(1)'s and New Forces, Nucl. Phys. B 347 (1990) 743–768. doi:10.1016/0550-3213(90)90381-M.
[19] D. Dunsky, L. J. Hall, K. Harigaya, CHAMP Cosmic Rays, JCAP 1907 (07) (2019) 015. arXiv:1812.11116, doi:10.1088/1475-7516/2019/07/015.
[20] S. D. McDermott, H.-B. Yu, K. M. Zurek, Turning off the Lights: How Dark is Dark Matter?, Phys. Rev. D 83 (2011) 063509. arXiv:1011.2907, doi:10.1103/PhysRevD.83.063509.
[21] M. Kachelrieß, J. Tjemsland, Reacceleration of charged dark matter, JCAP 10 (2020) 001. arXiv:2006.10479, doi:10.1088/1475-7516/2020/10/001.
[22] M. Fabbrichesi, E. Gabrielli, G. Lanfranchi, The Dark Photon (5 2020). arXiv:2005.01515.
[23] A. Filippi, M. De Napoli, Searching in the dark: the hunt for the dark photon, Rev. Phys. 5 (2020) 100042. arXiv:2006.04640, doi:10.1016/j.revip.2020.100042.
[24] J. D. Bowman, A. E. E. Rogers, R. A. Monsalve, T. J. Mozdzen, N. Mahesh, An absorption profile centred at 78 megahertz in the sky-averaged spectrum, Nature 555 (7694) (2018) 67–70. arXiv:1810.05912, doi:10.1038/nature25792.
[25] E. D. Kovetz, V. Poulin, V. Gluscevic, K. K. Boddy, R. Barkana, M. Kamionkowski, Tighter limits on dark matter explanations of the anomalous EDGES 21 cm signal, Phys. Rev. D 98 (10) (2018) 103529. arXiv:1807.11482, doi:10.1103/PhysRevD.98.103529.

[26] R. Engel, Photoproduction within the two component dual parton model. 1. Amplitudes and cross-sections, Z. Phys. C 66 (1995) 203–214. doi:10.1007/BF01496594.
[27] S. Roesler, R. Engel, J. Ranft, The Monte Carlo event generator DPMJET-III, in: International Conference on Advanced Monte Carlo for Radiation Physics, Particle Transport Simulation and Applications (MC 2000), 2000, pp. 1033–1038. arXiv:hep-ph/0012252, doi:10.1007/978-3-642-18211-2_166.
[28] A. Fedynitch, Cascade equations and hadronic interactions at very high energies, Ph.D. thesis, KIT, Karlsruhe, Dept. Phys. (11 2015). doi:10.5445/IR/1000055433.
[29] T. Sjöstrand, S. Ask, J. R. Christiansen, R. Corke, N. Desai, P. Ilten, S. Mrenna, S. Prestel, C. O. Rasmussen, P. Z. Skands, An introduction to PYTHIA 8.2, Comput. Phys. Commun. 191 (2015) 159–177. arXiv:1410.3012, doi:10.1016/j.cpc.2015.01.024.
[30] S. Ostapchenko, Monte Carlo treatment of hadronic interactions in enhanced Pomeron scheme: I. QGSJET-II model, Phys. Rev. D 83 (2011) 014018. arXiv:1010.1869, doi:10.1103/PhysRevD.83.014018.
[31] S. Ostapchenko, QGSJET-II: physics, recent improvements, and results for air showers, EPJ Web Conf. 52 (2013) 02001. doi:10.1051/epjconf/20125202001.
[32] F. Riehn, H. P. Dembinski, R. Engel, A. Fedynitch, T. K. Gaisser, T. Stanev, The hadronic interaction model SIBYLL 2.3c and Feynman scaling, PoS ICRC2017 (2018) 301. arXiv:1709.07227, doi:10.22323/1.301.0301.
[33] S. A. Bass, et al., Microscopic models for ultrarelativistic heavy ion collisions, Prog. Part. Nucl. Phys. 41 (1998) 255–369, [Prog. Part. Nucl. Phys.41,225(1998)]. arXiv:nucl-th/9803035, doi:10.1016/S0146-6410(98)00058-1.
[34] G. Agakishiev, et al., Inclusive dielectron spectra in p+p collisions at 3.5 GeV, Eur. Phys. J. A 48 (2012) 64. arXiv:1112.3607, doi:10.1140/epja/i2012-12064-y.
[35] M. Aguilar-Benitez, et al., Inclusive particle production in 400-GeV/c p p interactions, Z. Phys. C 50 (1991) 405–426. doi:10.1007/BF01551452.
[36] A. Baldini, V. Flaminio, W. G. Moorhead, D. R. O. Morrison, Total Cross-Sections for Reactions of High Energy Particles (Including Elastic, Topological, Inclusive and Exclusive Reactions) / Totale Wirkungsquerschnitte für Reaktionen hochenergetischer Teilchen (einschließlich elastischer,topologischer, inklusive), Vol. 12b of Landolt-Boernstein - Group I Elementary Particles, Nuclei and Atoms, Springer, 1988. doi:10.1007/b35211.
[37] A. Fedynitch, private communication.
[38] R. Engel, D. Heck, T. Pierog, Extensive air showers and hadronic interactions at high energy, Ann. Rev. Nucl. Part. Sci. 61 (2011) 467–489. doi:10.1146/annurev.nucl.012809.104544.
[39] K. Bays, et al., Supernova Relic Neutrino Search at Super-Kamiokande, Phys. Rev. D 85 (2012) 052007. arXiv:1111.5031, doi:10.1103/PhysRevD.85.052007.
[40] G. Magill, R. Plestid, M. Pospelov, Y.-D. Tsai, Millicharged particles in neutrino experiments, Phys. Rev. Lett. 122 (7) (2019) 071801. arXiv:1806.03310, doi:10.1103/PhysRevLett.122.071801.
[41] R. Acciarri, et al., Improved Limits on Millicharged Particles Using the ArgoNeuT Experiment at Fermilab, Phys. Rev. Lett. 124 (13) (2020) 131801. arXiv:1911.07996, doi:10.1103/PhysRevLett.124.131801.
[42] G. Alimonti, et al., The Borexino detector at the Laboratori Nazionali del Gran Sasso, Nucl. Instrum. Meth. A 600 (2009) 568–593. arXiv:0806.2400, doi:10.1016/j.nima.2008.11.076.
[43] A. A. Prinz, et al., Search for millicharged particles at SLAC, Phys. Rev. Lett. 81 (1998) 1175–1178. arXiv:hep-ex/9804008, doi:10.1103/PhysRevLett.81.1175.
[44] S. Chatrchyan, et al., Search for Fractionally Charged Particles in pp Collisions at $\sqrt{s} = 7$ TeV, Phys. Rev. D 87 (9) (2013) 092008. arXiv:1210.2311, doi:10.1103/PhysRevD.87.092008.
[45] S. Davidson, S. Hannestad, G. Raffelt, Updated bounds on millicharged particles, JHEP 05 (2000) 003. arXiv:hep-ph/0001179, doi:10.1088/1126-6708/2000/05/003.
[46] E. Golowich, R. W. Robinett, Limits on Millicharged Matter From Beam Dump Experiments, Phys. Rev. D 35 (1987) 391. doi:10.1103/PhysRevD.35.391.
[47] S. Davidson, B. Campbell, D. C. Bailey, Limits on particles of small electric charge, Phys. Rev. D 43

(1991) 2314–2321. doi:10.1103/PhysRevD.43.2314.
[48] P. Zyla, et al., Review of Particle Physics, PTEP 2020 (8) (2020) 083C01. doi:10.1093/ptep/ptaa104.
[49] L. G. Landsberg, Electromagnetic Decays of Light Mesons, Phys. Rept. 128 (1985) 301–376. doi:10.1016/0370-1573(85)90129-2.